J. Space Weather Space Clim., **6**, E01 (2016)
DOI: 10.1051/swsc/2016030

SWSC

PREFACE OPEN ACCESS

Scientific challenges in thermosphere-ionosphere forecasting – conclusions from the October 2014 NASA JPL community workshop

Anthony J. Mannucci[1,*], Maura E. Hagan[2], Angelos Vourlidas[3], Cheryl Y. Huang[4], Olga P. Verkhoglyadova[1], and Yue Deng[5]

[1] Jet Propulsion Laboratory, California Institute of Technology, Pasadena, CA 91109, USA
[*]Corresponding author: anthony.j.mannucci@jpl.nasa.gov
[2] Utah State University, Logan, UT 84322, USA
[3] Johns Hopkins University Applied Physics Laboratory, Laurel, MD 20723, USA
[4] Air Force Research Laboratory, Albuquerque, NM 87117, USA
[5] University of Texas at Arlington, Arlington, TX 76029, USA

Received 16 July 2015 / Accepted 22 August 2016

ABSTRACT

Interest in forecasting space weather in the thermosphere and ionosphere (T-I) led to a community workshop held at NASA's Jet Propulsion Laboratory in October, 2014. The workshop focus was "Scientific Challenges in Thermosphere-Ionosphere Forecasting" to emphasize that forecasting presumes a sufficiently advanced state of scientific knowledge, yet one that is still evolving. The purpose of the workshop, and this topical issue that arose from the workshop, was to discuss research frontiers that will lead to improved space weather forecasts. Three areas are discussed in some detail in this paper: (1) the role of lower atmosphere forcing in the response of the T-I to geomagnetic disturbances; (2) the significant deposition of energy at polar latitudes during geomagnetic disturbances; and (3) recent developments in understanding the propagation of coronal mass ejections through the heliosphere and prospects for forecasting the north-south component of the interplanetary magnetic field (IMF) using observations at the Lagrangian L_5 point. We describe other research presented at the workshop that appears in the topical issue. The possibility of establishing a "positive feedback loop" where improved scientific knowledge leads to improved forecasts is described (Siscoe 2006, *Space Weather*, **4**, S01003; Mannucci 2012, *Space Weather*, **10**, S07003).

Key words. Ionosphere (general) – Thermosphere – Storm – Interplanetary Coronal Mass Ejection (CME) – Heliosphere

1. Introduction

"Space weather" has become a prominent scientific paradigm. A central tenet of space weather is that scientific understanding can be achieved "sufficient for prediction" of space weather related phenomena (OFCM 2010). The possibility that scientific knowledge enables prediction of natural phenomena is a widely held opinion, certainly considered valid in the meteorological realm (Kalnay 2002). It is reasonable to expect that as scientific knowledge increases, prediction *accuracy* will generally increase also. Addressing scientific challenges to better understand the thermosphere-ionosphere system has both scientific and practical benefits.

This paper addresses a subset of scientific topics that, if better understood, will likely lead to improved forecasts of Earth's upper atmosphere – the thermosphere and ionosphere. The rest of the paper is organized as follows: in the next section, we discuss how science and forecasting are related. Then we discuss three scientific focus areas where progress will lead to improved prediction, that represent scientific forefront areas. We conclude with a summary and suggestions for future research directions.

2. Geospace science for improved forecasts

2.1 The role of data assimilation

The unique aspects of space weather need to be considered for determining the relevant science that leads to predictive capability. It is important to note that all types of weather forecast, space or terrestrial, rely on some form of data assimilation. This reliance comes about because forecasts are based on "first-principles" or "physics-based" general circulation models of the atmosphere, which computationally integrate systems of differential equations. The numerical outputs of atmospheric forecast models are sensitive to a significant degree to "boundary conditions" (or equivalently, "initial states") that are needed to integrate the dynamical equations. Data assimilation refers to setting boundary conditions or initial states based on actual measurements. Data assimilation is a prerequisite for accurate forecasts in the real world, as has been amply demonstrated in the meteorological realm.

A pioneering paper by Siscoe & Solomon (2006) identifies unique aspects of space weather forecasting that distinguish the data assimilation methods in space weather from those in terrestrial weather. They refer specifically to forecasts with lead times of one day or more, by analogy with terrestrial forecasts. Since such "medium-term" forecasts are the focus of an effort within the NASA Living With a Star (LWS) Partnership for Collaborative Space Weather Modeling (Mannucci et al. 2015a), Siscoe and Solomon's analysis is relevant to this effort. The central concept is contained in their Figure 1. This figure contains two axes: availability of data and sensitivity to boundary conditions. The point made is that in space weather, data availability is lower and sensitivity to boundary conditions is higher than it is for terrestrial weather. The higher sensitivity

to boundary conditions leads to a higher "compliance" of geospace, as described below.

It is clear from physical considerations that coupling of the thermosphere-ionosphere to external influences must be characterized to achieve accurate forecasts. Therefore, the T-I system is highly "compliant". As discussed in Siscoe & Solomon (2006), higher compliance systems tend to benefit less from data assimilation compared to systems that are more "persistent", such as terrestrial weather. However, the compliance of geospace applies to a single domain within the coupled Solar-Heliosphere-Earth system. Data assimilation's value to a forecast within the thermospheric domain, for example, may be of limited value during periods of significant forcing (e.g. geomagnetic storms). We note that a recent study by Chartier et al. (2013) suggests that even under strong forcing, data assimilation has value in the thermosphere for shorter term forecasts of about 6 h or so.

For forecasts with multiday lead times, our perspective must be that of a forecast originating at the solar corona. In that case, data assimilation in the solar domain is required, since magnetogram and other data are needed to initiate the solar heliospheric models that provide the forecasted drivers influencing the magnetosphere-thermosphere-ionosphere system (Merkin et al. 2007; Tóth et al. 2007; Mannucci et al. 2015a). The effectiveness of solar data assimilation may increase dramatically with spacecraft at the L_5 Lagrangian point, as discussed in Section 3.3.

Neither imaging from the L_5 point, nor advanced heliospheric models, have resolution sufficient to capture the smaller-scale Alfvénic fluctuations in the solar wind that are yet geo-effective (Solomon et al. 2012). Therefore, physics-based forecasting efforts should be augmented with data-driven models that can forecast the characteristics of the sub-grid scale fluctuations. One such effort, based on dynamical systems theory and applied to the geomagnetic AL index, is currently being developed and can model and predict sudden transitions in systems represented by time series data alone (Lynch et al. 2016). An approach that integrates data-driven techniques with the physics-based modeling approaches can be developed for the thermosphere-ionosphere system.

2.2 Coupling of the thermosphere-ionosphere to regions above and below

A useful science focus is on the coupling of the T-I system to regions above and below. A forefront science question directly relevant to forecasting is the degree to which the lower atmosphere modulates the response of the T-I to geomagnetic storms originating with the solar wind. At present, very little is known about this topic. The science is discussed in Section 3.1 of this paper. A finding is that storm-time response, e.g. of neutral temperature, may depend to a significant degree on forcing from the lower boundary. The response of the thermosphere to geomagnetic forcing depends on the prior thermospheric conditions, which are largely determined by driving from below (Hagan et al. 2015). Maute et al. (2015) recently addressed the question with simulations representative of the conditions during a sudden stratospheric warming (SSW) in 2013, during which geomagnetic and tidal forcing acted at the same time. Tidal forcing, which originates from below the T-I, was found to create comparable effects to geomagnetic forcing, although the relative influences varied with longitude. The recent work reported by Wang et al. (2016, this issue) bears on this problem because, for the first time, they have identified, not infrequently, ionospheric "anomalies" (see their paper for definition) that occur during geomagnetic quiet periods. We can speculate that at least a fraction of such anomalies are due to forcing from below and thus forcing from above and below are important elements of the full picture of "space weather". We expect that NASA's upcoming GOLD mission will improve this understanding substantially with "continuous staring" observations of thermospheric temperature on global scales during quiet and disturbed conditions.

Coupling from above, involving the magnetosphere and solar wind plasmas, is of course not a solved science topic. A useful focus is on understanding the energy transfer from the solar wind to the thermosphere-ionosphere system, via the magnetosphere as an intermediary. It has been shown that where the energy is deposited, as well as the quantity, has a large effect on the subsequent evolution of the T-I system (Deng & Ridley 2007; Matsuo & Richmond 2008). In the context of forecasting, energy can be viewed as a useful scalar quantity for which reasonably good quantitative estimates must be achieved to reach reasonable forecasts, and characterization must be improved if forecasts are to be improved (Verkhoglyadova et al. 2016, this issue).

Satellite measurements provide important insight into energy transfer into or out of the T-I system but are essentially point measurements that require interpolation and sophisticated intercalibration processing to make use of multiple satellite platforms. Examples of methods derived from satellite data are estimation of hemispheric power using DMSP and POES observations (Emery et al. 2006), or statistical models, e.g., estimations of auroral hemispheric power based on NOAA POES data (Fuller-Rowell & Evans 1987) or TIMED/GUVI observations (Zhang & Paxton 2008). The limited spatial coverage of satellite data limits the temporal and spatial scales of energy variability that we can analyze. This remains a problem that is likely to impact forecasting.

The altitude dependence of Joule heating via magnetospheric currents has a major impact on the neutral dynamics, which in turn affects the ionosphere to a substantial degree. Results presented at the workshop, based on the work of Huang et al. (2012), use simulations from the Thermosphere-Ionosphere Electrodynamics General Circulation Model (TIEGCM) to show that the global mean thermospheric temperature at 400 km altitude depends strongly on the altitude where the Joule heating occurs. Energy deposited in the E-region (altitude range 108–138 km) was compared with model runs where the same energy was deposited instead in the lower F-region (225–325 km). A key factor affecting the altitude distribution of Joule heating is the ionospheric Pedersen conductivity, which depends on the average energy of precipitating magnetospheric electrons during disturbed periods. Recent research by Sheng et al. (2014), using electron density profiles measured at high latitude by the FORMOSAT-3/COSMIC constellation, suggests that F-region Pedersen conductivity values used in TIECGM model runs are too low by a factor of 2, compared with E-region conductivities. Improved characterization of precipitating particle energies and fluxes, and thus Pedersen conductivities, would appear to be needed to improve the accuracy of forecasts.

While quantifying energy input from the solar wind and magnetosphere is a necessary task, it is not sufficient to

determine the T-I response. Huang et al. (2014 and Huang et al. 2016, this issue) discuss new findings which show that the polar cap is a location of significant energy input. However, community models are not sufficiently developed to capture significant amounts of energy entering through these "open" field lines. This suggests that a different sort of physics than dayside magnetic merging is responsible for a significant part of the T-I response, and may require a rethinking of how the solar wind coupling functions (Verkhoglyadova et al. 2016, this issue; Newell et al. 2007; Newell et al. 2008) are used to understand or forecast the T-I response.

Modeling is a tool to understand global as well as local energy transport processes (see e.g., Deng et al. 2011). However, questions that arise are: how well do we understand the underlying physics to adequately represent energy transport and how can we validate such modeling based on observations and empirical models. Since energy is the most general quantity conserved in a physical process, these questions are particularly important for forecasting the T-I system.

This issue (Connor et al. 2016) contains a case study of self-consistent coupling between a T-I model and a physics-based magnetospheric model, yielding improved estimates of auroral energy input and Joule heating compared to the more common empirically based magnetospheric inputs. In particular, during a period of enhanced solar wind dynamic pressure early in the storm (August 24, 2005), the physics-based OpenGGCM magnetosphere model coupled to the Coupled Thermosphere-Ionosphere Model (CTIM) leads to day-time high-latitude neutral density enhancements that compare better to observations than a T-I model coupled to empirically based auroral and electric field (convection) inputs. This suggests the promise of coupling magnetospheric and upper atmosphere models for forecasting purposes, although significantly more development is required, as pointed out in Connor et al. (2016).

2.3 Approaches to forecasting

It is worth reflecting on the fact that average patterns of storm-time response, particularly at specific locations and for ionospheric total electron content (TEC), have been known for decades (Mendillo 2006; Mendillo & Klobuchar 2006). That forecasting space weather, in particular TEC, remains a significant challenge suggests that in the upper atmosphere the average pattern is not representative of the actual patterns that occur from storm to storm. In other words, the variability between storms is quite significant (Prölss 1995; Mannucci et al. 2008; Prölss 2008; Buonsanto 1999; Mannucci et al. 2009; Borries et al. 2015) so that the information contained in a storm-time average pattern is important scientifically, but also somewhat limited as a predictive tool. The question of what causes variability of the storm-time behavior is fundamental and has no definitive scientific answer as yet. This, then, must represent a scientific frontier that the average pattern only addresses in a limited way.

A forecasting approach under development by Meng et al. (2016, this issue) demonstrates a link between scientific understanding and forecast accuracy. By analogy to numerical weather prediction (NWP), an ionospheric space weather forecast consists of the output of a global circulation model run, in this case the Global Ionosphere-Thermosphere Model (GITM, Ridley et al. 2006). To reduce the burden associated with evaluating the forecasts, the model computation is evaluated on a grid coarser than the native grid of the model: 30° × 15° for the evaluation versus 3.4° × 1° for the physics (longitude × latitude). As such, this approach explores a "coarse-grained" forecast. An even coarser evaluation approach was used by Chartier et al. (2013), which analyzed the mean electron density globally from the TIE-GCM. The resolution chosen by Meng et al. (2016) is sufficient to distinguish the physics in different physical regimes such as day/night, and low, middle, and high latitudes. These authors perform two steps supportive of the overall goal: first, they have extensive measurements for comparison with model output of at least one ionospheric quantity, the TEC. Second, they perform detailed evaluation of the model in terms of the physical factors leading to the modeled TEC. As the TEC is the by-product of multiple competing plasma production, loss and transport processes, the authors separately extract these factors from the model with a goal toward improved understanding of how these factors lead to the forecasted TEC.

A recent paper by Mannucci et al. (2015b) discusses the possibility of models producing output that agrees with observations (e.g. the TEC), although the models may contain insufficient physics. This is related to a common situation in geophysics: that cause and effect must be inferred without the benefit of controlled experiments. Forecasting, versus model validation using observations from the past, is less forgiving of situations where the model physics is insufficient. For this reason, forecasting as a component of the scientific process is useful because of the more stringent requirements it places on models.

3. Scientific focus areas

Although numerous areas are ripe for continued scientific exploration that are relevant to forecasting, we discuss the following three frontier science areas: (1) the role of lower atmosphere forcing in modifying the response to geomagnetic storms; (2) the location of energy deposition from the solar wind/magnetosphere; and (3) the possibility of forecasting B_z at Earth, a widely recognized need that is beginning to be addressed with concerted theoretical and observational approaches.

3.1 The role of lower atmosphere forcing in the T-I response to geomagnetic storms

The T-I system is in constant flux due to solar and geomagnetic forcing. Even during quiescent conditions, T-I variations persist over timescales of hours to days due to modest changes in high-latitude Joule heating and auroral precipitation sources. In recent years, an ever-growing body of observations has demonstrated that dynamical drivers originating in the lower and middle atmosphere also contribute to quiescent T-I variability in important ways (e.g., Immel et al. 2006; Hagan et al. 2007; Jin et al. 2008; Lühr et al. 2008; Oberheide & Forbes 2008; Forbes et al. 2009; Oberheide et al. 2009; Liu et al. 2010; Wan et al. 2010; He et al. 2011; Pedatella et al. 2012; Fang et al. 2013; Jones et al. 2013; Maute et al. 2014; Häusler et al. 2015) with practical consequences to satellite orbit prediction and communications capabilities. Thus, it is the aggregate effects of coupling from above and below that define the quiescent T-I variability and underlies the T-I response to solar geomagnetic storms.

Recently, Lu et al. (2015) demonstrated that the National Center for Atmospheric Research (NCAR)

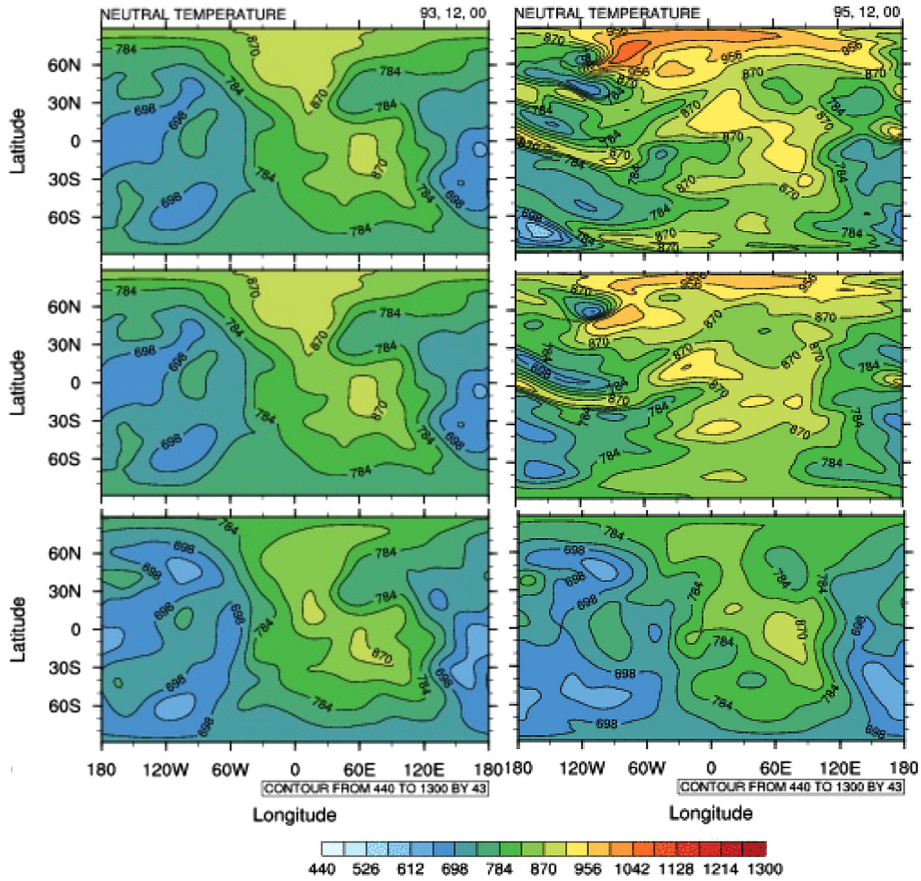

Fig. 1. Contours of neutral temperature (K) at 12:00 UT and 340 km altitude from an ensemble of TIME-GCM simulations on April 3, 2010 (left column) before the storm and during the storm on April 5, 2010 (right column) with optimal forcing (top row), constant lower boundary forcing (middle row), and constant upper boundary forcing (bottom row).

thermosphere-ionosphere-mesosphere-electrodynamics general circulation model (TIME-GCM) could capture the salient features of thermospheric observations made during the April 5, 2010 geomagnetic disturbance. TIME-GCM driven with observationally based time-dependent ionospheric convection and auroral precipitation patterns derived from the Assimilative Mapping of Ionospheric Electrodynamics (AMIE) procedure (after Richmond & Kamide 1988; Lu et al. 2015) reproduced the thermospheric winds observed by the Gravity field and steady-state Ocean Circulation Explorer (GOCE) and Challenging Minisatellite Payload (CHAMP) satellites, as well as the thermospheric densities from GOCE, CHAMP, and Gravity Recovery And Climate Experiment (GRACE) measurements. TIME-GCM runs driven by AMIE are used in the work described next as the basis for exploring the role of lower-boundary forcing in thermospheric variability during geomagnetic disturbances.

Hagan et al. (2015) diagnosed an ensemble of TIME-GCM simulations for the April 1–10, 2010 period to investigate the spatial and temporal variability of quiescent thermospheric temperature and zonal wind leading up to, during, and subsequent to the April 5 disturbance. Figure 1 exemplifies some of the neutral temperature variability that characterized the results from their TIME-GCM simulations. These latitude-longitude temperature maps are 12 UT snapshots at 340 km and illustrate the magnitude of some of the TIME-GCM temperature variability reported by Hagan et al. (2015). These maps complement and extend the results shown in Figure 2 of their report. The top panels are from their optimal TIME-GCM simulations driven by AMIE along with lower-boundary forcing given by the prevailing 10 hPa 3-hourly Modern-Era Retrospective Analysis for Research and Application (MERRA) zonal and meridional wind, temperature, and geopotential height reanalysis data (after Rienecker et al. 2011) from April 1–10, 2010. Temperature variability before the storm on April 3 (top left) is largely attributable to the variability in the absorption of solar radiation, which is modulated by atmospheric tides that propagate into the atmosphere from below. The day-to-day variability of the tides is evident in the bottom panels that illustrate TIME-GCM results from a diagnostic simulation with the same MERRA forcing but constant and quiescent upper-boundary forcing. There are notable differences in the details of the neutral temperature response during April 3 (bottom left) and 5 (bottom right) that are wholly attributable to the evolving lower boundary.

The middle and top panels in Figure 1 further illustrate how the variability of the thermospheric response to the geomagnetic disturbance is affected by tropospheric forcing. The middle panel results are from a diagnostic simulation with variable geomagnetic forcing, but constant lower-boundary forcing from MERRA that is the same between the quiet (left) and disturbed days (right). The top right panel is based on the same geomagnetic forcing as the middle right panel, but more realistic lower-boundary forcing. While the temperatures in the middle right panel capture salient features of the temperatures that are driven by the geomagnetic disturbance on April 5 (top right), there are also notable differences between the top and

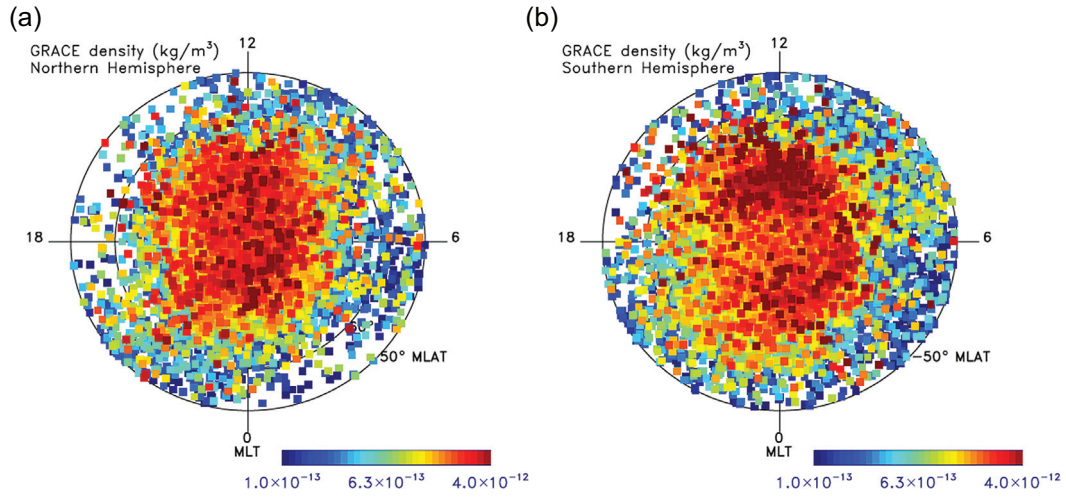

Fig. 2. Neutral density maxima (units of kg m^{-3}) extracted from GRACE observations, 2002–2012. Northern hemisphere maxima shown at (a), Southern hemisphere at (b).

middle right panels that are attributable to differences in lower-boundary forcing.

Figure 1 thus underscores the conclusions of Hagan et al. (2015) that the thermospheric response to any solar geomagnetic storm is predicated on the prevailing undisturbed thermospheric conditions. The global-scale spatial and temporal variability of these prevailing conditions is largely characterized by an aggregate of tidal and planetary wave oscillations, a significant component of which originates below the T-I system. This conclusion highlights the importance of accounting for the effects of dynamical forcing from below in an effort to develop accurate space weather forecasts of the T-I system.

3.2 Energy deposition at high latitudes

The large quantity of energy deposited in the upper atmosphere during storms has been known for decades, but there are several fundamental issues remaining to be understood. Among these are the spatial and temporal patterns of the deposition. The community has developed empirical and assimilative approaches to estimating such energy because it is a widely recognized need as a driver for global circulation models of the thermosphere-ionosphere. These same GCMs are the basis of space weather forecasts. The problem remains that a lack of observations, and poorly understood physical processes that determine patterns of energy deposition (e.g. magnetohydrodynamic versus kinetic physics), play significant roles.

It has recently been suggested that energy deposition in the polar cap, along open magnetic field lines, is underestimated in general (see Huang et al. 2016, this issue). In fact, maxima in neutral density caused by heat input have been found in the polar region for several storms. This is not the typical expectation and the implications in terms of global T-I modeling need to be better understood.

We have carried out a statistical analysis of neutral density maxima that occur at high latitudes as a result of energy deposition due to Poynting flux and energetic particle precipitation (Huang et al. 2016, this issue; see Figure 11). As shown by Huang et al. (2016), the thermospheric densities respond rapidly to the onset of magnetic activity. This response is exhibited as transient localized maxima in neutral density that we interpret as evidence of localized Joule heating. In our analysis, we apply a running mean to the neutral density observations and select maxima that are 30% above the mean. Over the 10 years since launch, the results of this analysis of GRACE neutral density data are shown in Figure 2. Summary statistics of the latitudes and magnetic local times of the density maxima are shown in Table 1 where the average, median and standard deviation of the mean are listed. It can be seen from Figure 2 that the density maxima occur at all local times in the polar cap and adjoining regions. A cluster of points appears in the Southern hemisphere centered at the nominal location of the cusp. A weak maximum in both hemispheres occurs between 11.5 and 12 MLT.

The significance of these results is that high-latitude energy deposition, despite its fundamental role in modifying the T-I during geomagnetic storms, is still not well understood. Huang et al. (2014) is the first study to point out that the polar cap may be a primary location of energy deposition, whereas previous studies have emphasized the cusp region and ignored the polar cap (Crowley et al. 2010; Knipp et al. 2011). Increased attention to this topic will not only improve our scientific understanding, but lead to improved T-I forecasts as well.

3.3 Forecasting interplanetary B_z at 1 AU

There is ample evidence that geomagnetic storms (Gonzalez & Tsurutani 1987; Tsurutani et al. 1995; Gonzalez et al. 1999) and even ionospheric TEC (Borries et al. 2015) are strongly connected to the north-south component (B_z) of the interplanetary magnetic field in the "vicinity" of Earth. More precisely, the correlation between geomagnetic activity and measured B_z at distances as large as 1.5×10^7 km from Earth is well established. An important component of a medium-range T-I forecast must be forecasting the orientation and time of arrival of B_z perturbations at Earth's magnetopause using models of the heliosphere and solar wind to propagate the CME characteristics (Zheng et al. 2013). There is mounting evidence that this difficult task is amenable to significant improvement using new observations and models. The current status is discussed next.

Research on coronal mass ejections (CMEs) and corotating interaction regions (CIRs), the drivers of Space Weather, has

Table 1. Statistics of neutral density maxima extracted from GRACE observations during 2002–2012. Statistics for the locations of the maxima in each hemisphere are shown for the full data set.

	MLat	MLT
NH		
Average	78.0287	11.8976
Median	79.7668	11.9107
Std. Dev.	7.1671	6.7125
SH		
Average	−74.7061	11.5906
Median	−75.7735	11.6888
Std. Dev.	7.4106	6.4352

undergone a revolution since the launch of the Solar Terrestrial Relations Observatory (STEREO; Kaiser et al. 2008). The mission is providing complete imaging coverage of the Sun-Earth line and three-dimensional measurements of CMEs/CIRs thanks to the imagers of the Sun-Earth Connection Coronal and Heliospheric Investigation (SECCHI; Howard et al. 2008). For the first time, we can measure the CME/CIR kinematics from Sun to Earth without gaps, study CME-CME and CME-solar wind interactions, and perform the first detailed comparisons between remote and in-situ observations of the *same* events. In addition, the sophistication of the magnetohydrodynamic (MHD) modeling of CME propagation has increased in tandem with the relentless gains in computing capability. Ensemble modeling of CMEs, although still in its infancy, is now possible (Lee et al. 2013).

Naturally, ongoing research has direct implications on important Space Weather issues, such as:

1. The realization that fast solar wind streams can trap small CMEs, or rather magnetic flux ropes (MFRs), thus enhancing their geo-effectiveness (Rouillard et al. 2009).
2. CMEs may rotate and deflect during their propagation in the inner heliosphere (Vourlidas et al. 2011; Isavnin et al. 2013, 2014).
3. The CME-driven shock can be detected routinely (Vourlidas et al. 2013; Kwon et al. 2015) and is used to provide estimates of the interplanetary magnetic field upstream of the CME (e.g. Poomvises et al. 2010).
4. More importantly, the availability of kinematics measurements beyond 30 solar radii (the upper limit before STEREO) improves predictions for the CME Time of Arrival (ToA) from about 24 h to ±6–8 h (Colaninno et al. 2013, Millward et al. 2013).
5. CME-CME interaction can considerably affect the geo-effectiveness of an event by reducing aerodynamic drag (Temmer & Nitta 2015), enhancing particle acceleration (Lario & Karelitz 2014), or by strengthening the shock (Lugaz et al. 2005).
6. Finally, we have the first attempts to estimate the CME B_z (Kunkel & Chen 2010; Savani et al. 2015) based on combinations of modeling and heliospheric observations.

There remain, however, several open questions (e.g. Zhao & Dryer 2014). For example, ToA predictions for individual events can be off by several hours (Colaninno et al. 2013; Möstl et al. 2014). The reason is likely our inaccurate modeling of the background solar wind, which relies on boundary conditions of 27-day averaged photospheric magnetic field information. Analyses of CME-CME interaction are challenging beyond ~50 solar radii because of the lower spatial resolution of the images and the confusion from overlapping structures along the line of sight. The comparisons between remote sensing and *in-situ* remain inconsistent, especially in regard to the orientation or shape of the CME (e.g. Nieves-Chinchilla et al. 2012). The discrepancies affect the reliability of studies on CME deflection/rotation and generally dynamic evolution. And of course, we are still unable to reliably predict B_z, the most sought-after geo-effective solar wind parameter.

These problems can, however, be addressed with the proper mixture of observations and modeling. The answers lie in better understanding of: (1) the CME interaction with the ambient solar wind, including CME shocks, (2) the relationship of structures in images with structures measured *in-situ*, and (3) the connection between low coronal manifestations of erupting activity and the eventual CME. As STEREO has demonstrated, "off-Sun-Earth-line" imaging is key with the L_4/L_5 Lagrangian points, the optimal location for such studies (Webb et al. 2010; Gopalswamy et al. 2011; Vourlidas 2015). Magnetograph observations from L_5 will be especially beneficial to modeling and space weather forecasting. The essential boundary condition for all heliospheric modeling is the photospheric field (magnitude, direction) over the full solar surface. Since only the Earth-facing part of the disk is currently observed, full surface maps must be constructed by averages over the 27-day rotation period of the Sun. Therefore, the oldest observations concern the field just behind the East solar limb. Hence, magnetograph observations from L_5 will directly address one of the major weaknesses of current modeling by delivering observations of the field at those eastern longitudes. When combined with Earth-based observations, information from observations will extend over about two-thirds of the surface, thus dramatically increasing the reliability of all heliospheric modeling (Vourlidas 2015). Better initial conditions lead to better modeling of the background solar wind and will improve studies of CME-solar wind interactions and the accuracy of ToA predictions.

As for B_z, we expect significant improvements in the existing methodologies, and the introduction of new methodologies, thanks to the sustained observations of pre-erupting structures, such as the recently discovered hot MFRs (e.g. Zhang et al. 2012; Patsourakos et al. 2013), Earth-directed CMEs (both structures seen on the limb from L_4/L_5), combined with extrapolations of the photospheric field (now accurately measured over a large fraction of the disk) and the improved propagation models.

4. Summary and conclusions

The scientific problems unique to space weather forecasts with lead times of a few days are best addressed in the context of performing such forecasts. A community workshop held at NASA's Jet Propulsion Laboratory in October, 2014 focused on such scientific challenges using resources such as general circulation models of the thermosphere-ionosphere and ground and space-based observations. The potential lack of accuracy of numerical space weather predictions that might be attempted now, due to uncertainties in the physical prediction chain originating at the solar corona, should not preclude a scientific focus on forecasting. At any time in the evolution of a scientific field, there will be boundaries to our understanding. *Of immediate value is establishing a useful link between*

scientific understanding and forecast accuracy. While there are certain to be fundamental limits to "predictability" in the sense of sensitivity to initial conditions (e.g. chaos), the degree to which chaos may limit space weather forecasting is not known. A component of space weather research should therefore focus on how limited scientific knowledge is limiting the accuracy of forecasts. Developing concrete approaches to improve such knowledge via observations, theory, and modeling is desirable. Understanding the sources of variability of the magnetosphere-thermosphere-ionosphere system is paramount.

In this paper, we discuss three specific science areas that are relevant to forecasting T-I space weather: (1) the role of lower atmosphere forcing; (2) deposition of energy at polar latitudes during geomagnetic disturbances; and (3) propagation of coronal mass ejections through the heliosphere. All three areas (among others) were discussed at the 2014 workshop held at JPL. Simulations using the TIME-GCM model strongly suggest that conditions before the onset of a geomagnetic storm have significant influence on the storm's impact, which leads to the conclusion that terrestrial weather patterns that modulate tidal forcing of the thermosphere will influence storm-time dynamics (Hagan et al. 2015; Lu et al. 2015). However, the relationship between terrestrial and space weather is not well represented in the literature at this time. A novel approach to assessing ionospheric variability (Wang et al. 2016) demonstrates that variability is not always associated with geomagnetically active periods. This may be a signature of lower atmosphere forcing and is deserving of further study.

The role of energy deposition during geomagnetic storms has recently been studied using satellite observations of electromagnetic and neutral density perturbations (Huang et al. 2014, 2016). Energy deposition in the polar cap, versus auroral latitudes, is found to be a significant and possibly dominant phenomenon during storms, with major implications for global thermosphere circulation patterns and the evolution of ionospheric storms.

Runs of the GITM global circulation model were assessed in "forecast mode" to be driven by solar wind parameters that in principle could be forecast several days in advance (Meng et al. 2016). Similar runs were evaluated to trace the flow of energy from high to low latitudes during storms (Verkhoglyadova et al. 2016). These authors find that establishing the connection between improved scientific knowledge and improved forecasts requires detailed analysis of the GCMs used to perform the forecasts, and detailed comparisons with observations. Such comprehensive model evaluations will benefit both forecasting and science, and represents a frontier area in the use of numerical models for scientific investigations (Mannucci et al. 2015b).

Of course, accurate forecasts of the T-I will ultimately be predicated on what can be achieved regarding forecasts of solar wind conditions at Earth's magnetopause. Recent research in this area is promising. Observations from the STEREO spacecraft have demonstrated that imaging coverage of the Sun-Earth line without gaps, combined with sophisticated MHD modeling of CME propagation through the heliosphere, offers significant possibilities to forecast time of arrival of solar wind disturbances with uncertainties less than six hours. STEREO has demonstrated that a spacecraft located at the L_4 or L_5 Lagrange points between sun and Earth are excellent vantage points for solar wind observations, making space weather forecasts with multiday lead times a practical possibility if sufficient observational resources are available.

Acknowledgements. Portions of this research were carried out at the Jet Propulsion Laboratory, California Institute of Technology, under a contract with the National Aeronautics and Space Administration. Sponsorship of the NASA/NSF Partnership for Collaborative Space Weather Modeling is gratefully acknowledged. MH thanks K. Häusler for the TIME-GCM figures. MH was supported by the National Center for Atmospheric Research (NCAR) under the sponsorship of the National Science Foundation (NSF) and by the U.S. Participating Investigator (USPI) Program under NASA Grant NNX12AD26G. AV was supported by internal APL funds. CH acknowledges the support of the Air Force Office of Scientific Research under Grant LRIR 14 RV11COR.

References

Borries, C., J. Berdermann, N. Jakowski, and V. Wilken. Ionospheric storms – a challenge for empirical forecast of the total electron content. *J. Geophys. Res. [Space Phys.]*, **120 (4)**, 3175–3186, 2015, DOI: 10.1002/2015ja020988.

Buonsanto, M. Ionospheric storms – a review. *Space Sci. Rev.*, **88 (3–4)**, 563–601, 1999, DOI: 10.1023/A:1005107532631.

Chartier, A.T., D.R. Jackson, and C.N. Mitchell. A comparison of the effects of initializing different thermosphere-ionosphere model fields on storm time plasma density forecasts. *J. Geophys. Res. [Space Phys.]*, **118 (11)**, 7329–7337, 2013, DOI: 10.1002/2013JA019034.

Colaninno, R.C., A. Vourlidas, and C.C. Wu. Quantitative comparison of methods for predicting the arrival of coronal mass ejections at Earth based on multiview imaging. *J. Geophys. Res. [Space Phys.]*, **118 (11)**, 6866–6879, 2013, DOI: 10.1002/2013JA019205.

Connor, H.K., E. Zesta, M. Fedrizzi, Y. Shi, J. Raeder, M.V. Codrescu, and T.J. Fuller-Rowell. Modeling the ionosphere-thermosphere response to a geomagnetic storm using physics-based magnetospheric energy input: OpenGGCM-CTIM results. *J. Space Weather Space Clim.*, **6**, A25, 2016, DOI: 10.1051/swsc/2016019.

Crowley, G., D.J. Knipp, K.A. Drake, J. Lei, E. Sutton, and H. Luhr. Thermospheric density enhancements in the dayside cusp region during strong B-Y conditions. *Geophy. Res. Lett.*, **37**, L07110, 2010, DOI: 10.1029/2009gl042143.

Deng, Y., and A.J. Ridley. Possible reasons for underestimating Joule heating in global models: E field variability, spatial resolution, and vertical velocity. *J. Geophys. Res. [Space Phys.]*, **112(A)**, A09308, 2007, DOI: 10.1029/2006JA012006.

Deng, Y., Y. Huang, J. Lei, A.J. Ridley, R. Lopez, and J. Thayer. Energy input into the upper atmosphere associated with high-speed solar wind streams in 2005. *J. Geophys. Res. Space Phys.*, **116**, A05303, 2011, DOI: 10.1029/2010JA016201.

Emery, B.A., D.S. Evans, M.S. Greer, E. Holeman, K. Kadinsky-Cade, F.J. Rich, and W. Xu. The low energy auroral electron and ion hemispheric power after NOAA and DMSP intersatellite adjustments. NCAR Technical Note, NCAR/TN-470+STR, HAO/NCAR, 2006.

Fang, T.-W., R. Akmaev, T. Fuller-Rowell, F. Wu, N. Maruyama, and G. Millward. Longitudinal and day-to-day variability in the ionosphere from lower atmosphere tidal forcing. *Geophys. Res. Lett.*, **40**, 2523–2528, 2013, DOI: 10.1002/grl.50.

Forbes, J.M., S.L. Bruinsma, X. Zhang, and J. Oberheide. Surface-exosphere coupling due to thermal tides. *Geophys. Res. Lett.*, **36**, L15812, 2009, DOI: 10.1029/2009GL03874.

Fuller-Rowell, T.J., and D.S. Evans. Height-integrated Pedersen and Hall conductivity patterns inferred from the TIROS/NOAA satellite data. *J. Geophys. Res. [Space Phys.]*, **92**, 7606–7618, 1987, DOI: 10.1029/JA092iA07p07606.

Gonzalez, W.D., and B.T. Tsurutani. Criteria of interplanetary parameters causing intense magnetic storms (Dst less-than −100 nT). *Planet. Space Sci.*, **35 (9)**, 1101–1109, 1987, DOI: 10.1016/0032-0633(87)90015-8.

Gonzalez, W.D., B.T. Tsurutani, and A.L.C. De Gonzalez. Interplanetary origin of geomagnetic storms. *Space Sci. Rev.*, **88 (3–4)**, 529–562, 1999, DOI: 10.1023/a:1005160129098.

Gopalswamy, N., J.M. Davila, O.C. St. Cyr, E.C. Sittler, F. Auchère, et al. Earth-Affecting Solar Causes Observatory (EASCO): a potential international living with a star mission from Sun–Earth L5. *J. Atmos. Sol. Terr. Phys.*, **73 (5–6)**, 658–663, 2011, DOI: 10.1016/j.jastp.2011.01.013.

Hagan, M.E., A. Maute, R.G. Roble, A.D. Richmond, T.J. Immel, and S.L. England. Connections between deep tropical clouds and the Earth's ionosphere. *Geophys. Res. Lett.*, **34**, L20109, 2007, DOI: 10.1029/2007GL030142.

Hagan, M.E., K. Haeusler, G. Lu, J.M. Forbes, and X. Zhang. Upper thermospheric responses to forcing from above and below during 1–10 April 2010: results from an ensemble of numerical simulations. *J. Geophys. Res. [Space Phys.]*, **120 (4)**, 3160–3174, 2015, DOI: 10.1002/2014ja020706.

Häusler, K., M.E. Hagan, J.M. Forbes, X. Zhang, E. Doornbos, S. Bruinsma, and G. Lu. Intraannual variability of tides in the thermosphere from model simulations and in situ satellite observations. *J. Geophys. Res. [Space Phys.]*, **120 (1)**, 751–765, 2015, DOI: 10.1002/2014JA020579.

He, M., L. Liu, W. Wan, and Y. Wei. Strong evidence for couplings between the ionospheric wave-4 structure and atmospheric tides. *Geophys. Res. Lett.*, **38**, L14101, 2011, DOI: 10.1029/2011GL047855.

Howard, R.A., et al.. Sun Earth Connection Coronal and Heliospheric Investigation (SECCHI). *Space Sci. Rev.*, **136 (1)**, 67–115, 2008, DOI: 10.1007/s11214-008-9341-4.

Huang, Y., A.D. Richmond, Y. Deng, and R. Roble. Height distribution of Joule heating and its influence on the thermosphere. *J. Geophys. Res. [Space Phys.]*, **117**, A08334, 2012, DOI: 10.1029/2012JA017885.

Huang, C.Y., Y.J. Su, E.K. Sutton, D.R. Weimer, and R.L. Davidson. Energy coupling during the August 2011 magnetic storm. *J. Geophys. Res. [Space Phys.]*, **119 (2)**, 1219–1232, 2014, DOI: 10.1002/2013ja019297.

Huang, C.Y.-Y., Y. Huang, Y.-J. Su, E.K. Sutton, M.R. Hairston, and W.R. Coley. Ionosphere-thermosphere (IT) response to solar wind forcing during magnetic storms. *J. Space Weather Space Clim.*, **6**, A4, 2016, DOI: 10.1051/swsc/2015041.

Immel, T.J., E. Sagawa, S.L. England, S.B. Henderson, M.E. Hagan, S.B. Mende, H.U. Frey, C.M. Swenson, and L.J. Paxton. The control of equatorial ionospheric morphology by atmospheric tides. *Geophys. Res. Lett.*, **33 (15)**, L15108, 2006, DOI: 10.1029/2006GL026161.

Isavnin, A., A. Vourlidas, and E.K.J. Kilpua. Three-dimensional evolution of erupted flux ropes from the Sun (2–20 R ☉) to 1 AU. *Sol. Phys.*, **284 (May 1)**, 203–215, 2013, DOI: 10.1007/s11207-012-0214-3.

Isavnin, A., A. Vourlidas, and E.K.J. Kilpua. Three-dimensional evolution of flux-rope CMEs and its relation to the local orientation of the heliospheric current sheet. *Sol. Phys.*, **289 (6)**, 2141–2156, 2014, DOI: 10.1007/s11207-013-0468-4.

Jin, H., Y. Miyoshi, H. Fujiwara, and H. Shinagawa. Electrodynamics of the formation of ionospheric wave number 4 longitudinal structure. *J. Geophys. Res. [Space Phys.]*, **113**, A09307, 2008, DOI: 10.1029/2008JA013301.

Jones Jr., M., J.M. Forbes, M.E. Hagan, and A. Maute. Non-migrating tides in the ionosphere-thermosphere: in-situ versus tropospheric sources. *J. Geophys. Res. [Space Phys.]*, **118**, 2438–2451, 2013, DOI: 10.1002/jgra.50257.

Kaiser, M.L., T.A. Kucera, J.M. Davila, O.C.S. Cyr, M. Guhathakurta, and E. Christian. The STEREO mission: an introduction. *Space Sci. Rev.*, **136 (1)**, 5–16, 2008, DOI: 10.1007/s11214-007-9277-0.

Kalnay, E. *Atmospheric modeling, data assimilation and predictability*, Cambridge University Press, NY, ISBN: 978-0521796293, 2002.

Knipp, D., S. Eriksson, L. Kilcommons, G. Crowley, J. Lei, M. Hairston, and K. Drake. Extreme Poynting flux in the dayside thermosphere: examples and statistics. *Geophys. Res. Lett.*, **38**, L16102, 2011, DOI: 10.1029/1022GL048302.

Kunkel, V., and J. Chen. Evolution of a coronal mass ejection and its magnetic field in interplanetary space. *ApJ Lett.*, **715 (2)**, L80–L83, 2010, DOI: 10.1088/2041-8205/715/2/L80.

Kwon, R.-Y., J. Zhang, and A. Vourlidas. Are halo-like solar coronal mass ejections merely a matter of geometric projection effects? *ApJ Lett.*, **799 (2)**, L29 (5 pp), 2015, DOI: 10.1088/2041-8205/799/2/L29.

Lario, D., and A. Karelitz. Influence of interplanetary coronal mass ejections on the peak intensity of solar energetic particle events. *J. Geophys. Res. [Space Phys.]*, **119 (6)**, 4185–4209, 2014, DOI: 10.1002/2014JA019771.

Lee, C.O., C.N. Arge, D. Odstrčil, G. Millward, V. Pizzo, J.M. Quinn, and C.J. Henney. Ensemble modeling of CME propagation. *Sol. Phys.*, **285**, 349–368, 2013, DOI: 10.1007/s11207-012-9980-1.

Liu, H.-L., W. Wang, A.D. Richmond, and R.G. Roble. Ionospheric variability due to planetary waves and tides for solar minimum conditions. *J. Geophys. Res. [Space Phys.]*, **115**, A00G01, 2010, DOI: 10.1029/2009JA015188.

Lu, G., M. Hagan, K. Häusler, E. Doornbos, S. Bruinsma, B.J. Anderson, and H. Korth. Global ionospheric and thermospheric response to the 5 April 2010 geomagnetic storm: an integrated data-model investigation. *J. Geophys. Res. [Space Phys.]*, **119**, 10358–10375, 2015, DOI: 10.1002/2014JA020555.

Lugaz, N., W.B.I. Manchester, and T.I. Gombosi. Numerical simulation of the interaction of two coronal mass ejections from Sun to Earth. *ApJ*, **634 (1)**, 651–662, 2005, DOI: 10.1086/491782.

Lühr, H., M. Rother, K. Häusler, P. Alken, and S. Maus. The influence of nonmigrating tides on the longitudinal variation of the equatorial electrojet. *J. Geophys. Res. [Space Phys.]*, **113**, A08313, 2008, DOI: 10.1029/2008JA01.

Lynch, E., D. Kaufman, A.S. Sharma, E. Kalnay, and K. Ide. Brief Communication: breeding vectors in the phase space reconstructed from time series data. *Nonlin. Proc. Geophys.*, **23 (3)**, 137–141, 2016, DOI: 10.5194/npg-23-137-2016.

Mannucci, A.J. Charting a path toward improved space weather forecasting. *Space Weather*, **10**, S07003, 2012, DOI: 10.1029/2012SW000819.

Mannucci, A.J., B.T. Tsurutani, M.A. Abdu, W.D. Gonzalez, A. Komjathy, E. Echer, B.A. Iijima, G. Crowley, and D. Anderson. Superposed epoch analysis of the dayside ionospheric response to four intense geomagnetic storms. *J. Geophys. Res. [Space Phys.]*, **113**, A00A02, 2008, DOI: 10.1029/2007JA012732.

Mannucci, A.J., B.T. Tsurutani, M.C. Kelley, B.A. Iijima, and A. Komjathy. Local time dependence of the prompt ionospheric response for the 7, 9, and 10 November 2004 superstorms. *J. Geophys. Res. [Space Phys.]*, **114**, A10308, 2009, DOI: 10.1029/2009JA014043.

Mannucci, A.J., O.P. Verkhoglyadova, B.T. Tsurutani, X. Meng, X. Pi, et al. Medium-range thermosphere-ionosphere storm forecasts. *Space Weather*, **13 (3)**, 125–129, 2015a, DOI: 10.1002/2014sw001125.

Mannucci, A.J., B.T. Tsurutani, O.P. Verkhoglyadova, and X. Meng. On scientific inference in geophysics and the use of numerical simulations for scientific investigations. *Earth Space Sci.*, **2 (8)**, 359–367, 2015b, DOI: 10.1002/2015EA000108.

Matsuo, T., and A.D. Richmond. Effects of high-latitude ionospheric electric field variability on global thermospheric Joule heating and mechanical energy transfer rate. *J Geophys. Res. [Space Phys.]*, **113 (A7)**, A07309, 2008, DOI: 10.1029/2007ja012993.

Maute, A., M.E. Hagan, A.D. Richmond, and R.G. Roble. TIME-GCM study of the ionospheric equatorial vertical drift changes during the 2006 Stratospheric Sudden Warming. *J. Geophys. Res. [Space Phys.]*, **119**, 1287–1305, 2014, DOI: 10.1002/2013JA019490.

Maute, A., M.E. Hagan, V. Yudin, H.-L. Liu, and E. Yizengaw. Causes of the longitudinal differences in the equatorial vertical E × B drift during the 2013 SSW period as simulated by the TIME-GCM. *J. Geophys. Res. [Space Phys.]*, **120**, 5117–5136, 2015, DOI: 10.1002/2015JA021126.

Mendillo, M. Storms in the ionosphere: patterns and processes for total electron content. *Rev. Geophys.*, **44**, RG4001, 2006, DOI: 10.1029/2005RG000193.

Mendillo, M., and J.A. Klobuchar. Total electron content: synthesis of past storm studies and needed future work. *Radio Sci.*, **41**, RS5S02, 2006, DOI: 10.1029/2005RS003394.

Meng, X., A.J. Mannucci, O.P. Verkhoglyadova, and B.T. Tsurutani. On forecasting ionospheric total electron content responses to high-speed solar wind streams. *J. Space Weather Space Clim.*, **6**, A19, 2016, DOI: 10.1051/swsc/2016014.

Merkin, V.G., M.J. Owens, H.E. Spence, W.J. Hughes, and J.M. Quinn. Predicting magnetospheric dynamics with a coupled Sun-to-Earth model: challenges and first results. *Space Weather*, **5**, S12001, 2007, DOI: 10.1029/2007sw000335.

Millward, G., D. Biesecker, V. Pizzo, and C.A. de Koning. An operational software tool for the analysis of coronagraph images: determining CME parameters for input into the WSA-Enlil heliospheric model. *Space Weather*, **11**, 57–68, 2013, DOI: 10.1002/swe.20024.

Möstl, C., K. Amla, J.R. Hall, P.C. Liewer, E.M. De Jong, et al. Connecting speeds, directions and arrival times of 22 coronal mass ejections from the Sun to 1 AU. *ApJ*, **787 (2)**, 119, 2014, DOI: 10.1088/0004-637X/787/2/119.

Newell, P.T., T. Sotirelis, K. Liou, C.-I. Meng, and F.J. Rich. A nearly universal solar wind-magnetosphere coupling function inferred from 10 magnetospheric state variables. *J. Geophys. Res. [Space Phys.]*, **112**, A01206, 2007, DOI: 10.1029/2006JA012015.

Newell, P.T., T. Sotirelis, K. Liou, and F.J. Rich. Pairs of solar wind-magnetosphere coupling functions: combining a merging term with a viscous term works best. *J. Geophys. Res. [Space Phys.]*, **113**, A04218, 2008, DOI: 10.1029/2007JA012825.

Nieves-Chinchilla, T., R. Colaninno, A. Vourlidas, A. Szabo, R.P. Lepping, S.A. Boardsen, B.J. Anderson, and H. Korth. Remote and in situ observations of an unusual earth-directed coronal mass ejection from multiple viewpoints. *J. Geophys. Res.*, **117**, A06106, 2012, DOI: 10.1029/2011JA017243.

Oberheide, J., and J.M. Forbes. Tidal propagation of deep tropical cloud signatures into the thermosphere from TIMED observations. *Geophys. Res. Lett.*, **35**, L04816, 2008, DOI: 10.1029/2007GL032397.

Oberheide, J., J.M. Forbes, K. Häusler, Q. Wu, and S.L. Bruinsma. Tropospheric tides from 80 to 400 km: Propagation, interannual variability, and solar cycle effects. *J. Geophys. Res.*, **114**, D00I05, 2009, DOI: 10.1029/2009JD0.

OFCM. "The National Space Weather Program Strategic Plan", National Space Weather Program Council, Office of the Federal Coordinator for Meteorological Services and Supporting Research, Document FCM-P30-2010, Washington, DC, 2010

Patsourakos, S., A. Vourlidas, and G. Stenborg. Direct evidence for a fast coronal mass ejection driven by the prior formation and subsequent destabilization of a magnetic flux rope. *ApJ*, **764**, 125, 2013, DOI: 10.1088/0004-637X/764/2/125.

Pedatella, N.M., M.E. Hagan, and A. Maute. The comparative importance of DE3, SE2, and SPW4 on the generation of wavenumber-4 longitude structures in the low-latitude ionosphere during September equinox. *Geophys. Res. Lett.*, **39**, L19108, 2012, DOI: 10.1029/2012GL053643.

Poomvises, W., J. Zhang, and O. Olmedo. Coronal mass ejection propagation and expansion in three-dimensional space in the heliosphere based on STEREO/SECCHI observations. *ApJ Lett.*, **717**, L159–L163, 2010, DOI: 10.1088/2041-8205/717/2/L159.

Prölss, G.W., Ionospheric F-region storms. In: H., Volland, Editor. *Handbook of Atmospheric Electrodynamics*, **vol. 2**, CRC Press, Boca Raton, FL, 195–235, 1995.

Prölss, G.W., Ionospheric storms at mid-latitude: A short review. In: M. Paul Kintner Jr., J. Anthea Coster, T. Fuller-Rowell, J. Anthony Mannucci, M. Mendillo, and R. Heelis, Editors. *Midlatitude Ionospheric Dynamics and Disturbances, Geophys. Monogr. Ser. 181*, AGU Geophysical Monograph Series, **vol. 181**, AGU, Washington, DC, 9–24, ISBN: 978-0-87590-446-7, 2008, DOI: 10.1029/181GM03.

Richmond, A.D., and Y. Kamide. Mapping electrodynamic features of the high-latitude ionosphere from localized observations: technique. *J. Geophys. Res. [Space Phys.]*, **93 (A6)**, 5741–5759, 1988, DOI: 10.1029/JA093iA06p05741.

Ridley, A.J., Y. Deng, and G. Tóth. The global ionosphere-thermosphere model. *J. Atmos. Sol. Terr. Phys.*, **68**, 839–864, 2006, DOI: 10.1016/j.jastp.2006.01.008.

Rienecker, M.M., M.J. Suarez, R. Gelaro, R. Todling, J. Bacmeister, et al. MERRA: NASA's modern-era retrospective analysis for research and applications. *J. Clim.*, **24 (14)**, 3624–3648, 2011, DOI: 10.1175/JCLI-D-11-00015.1.

Rouillard, A.P., N.P. Savani, J.A. Davies, B. Lavraud, R.J. Forsyth, et al. A multispacecraft analysis of a small-scale transient entrained by solar wind streams. *Sol. Phys*, **256 (1)**, 307–326, 2009, DOI: 10.1007/s11207-009-9329-6.

Savani, N.P., A. Vourlidas, A. Szabo, M.L. Mays, I.G. Richardson, B.J. Thompson, A. Pulkkinen, R. Evans, and T. Nieves-Chinchilla. Predicting the magnetic vectors within coronal mass ejections arriving at Earth: 1. Initial architecture. *Space Weather*, **13 (6)**, 374–385, 2015, DOI: 10.1002/2015SW001171.

Sheng, C., Y. Deng, X. Yue, and Y. Huang. Height-integrated Pedersen conductivity in both E and F regions from COSMIC observations. *J. Atmos. Sol. Terr. Phys.*, **115–116C**, 79–86, 2014, DOI: 10.1016/j.jastp.2013.12.013.

Siscoe, G. A culture of improving forecasts: lessons from Meteorology. *Space Weather*, **4**, S01003, 2006, DOI: 10.1029/2005SW000178.

Siscoe, G., and S.C. Solomon. Aspects of data assimilation peculiar to space weather forecasting. *Space Weather*, **4 (4)**, S04002, 2006, DOI: 10.1029/2005SW000205.

Solomon, S.C., A.G. Burns, B.A. Emery, M.G. Mlynczak, L. Qian, W. Wang, D.R. Weimer, and M. Wiltberger. Modeling studies of the impact of high-speed streams and co-rotating interaction regions on the thermosphere-ionosphere. *J. Geophys. Res. [Space Phys.]*, **117**, A00L11, 2012, DOI: 10.1029/2011JA017417.

Temmer, M., and N.V. Nitta. Interplanetary propagation behavior of the fast coronal mass ejection on 23 July 2012. *Sol. Phys.*, **290 (3)**, 919–932, 2015, DOI: 10.1007/s11207-014-0642-3.

Tóth, G., D.L. De Zeeuw, T.I. Gombosi, W.B. Manchester, A.J. Ridley, I.V. Sokolov, and I.I. Roussev. Sun-to-thermosphere simulation of the 28–30 October 2003 storm with the space weather modeling framework. *Space Weather*, **5 (6)**, S06003, 2007, DOI: 10.1029/2006sw000272.

Tsurutani, B.T., W.D. Gonzalez, A.L.C. Gonzalez, F. Tang, J.K. Arballo, and M. Okada. Interplanetary origin of geomagnetic activity in the declining phase of the solar cycle. *J Geophys. Res. [Space. Phys.]*, **100 (A11)**, 21717–21734, 1995, DOI: 10.1029/95JA01476.

Verkhoglyadova, O., X. Meng, A.J. Mannucci, B.T. Tsurutani, L.A. Hunt, M.G. Mlynczak, R. Hajra, and B.A. Emery. Estimation of energy budget of ionosphere-thermosphere system during two CIR-HSS events: observations and modeling. *J. Space Weather Space Clim.*, **6**, A20–A22, 2016, DOI: 10.1051/swsc/2016013.

Vourlidas, A. Mission to the Sun-Earth L5 Lagrangian point: an optimal platform for space weather research. *Space Weather*, **13**, 197–201, 2015, DOI: 10.1002/2015SW001173.

Vourlidas, A., R. Colaninno, T. Nieves-Chinchilla, and G. Stenborg. The first observation of a rapidly rotating coronal mass ejection in the middle corona. *ApJ* **733 (2)**, L23, 2011, DOI: 10.1088/2041-8205/733/2/L23.

Vourlidas, A., B.J. Lynch, R.A. Howard, and Y. Li. How many CMEs have flux ropes? Deciphering the signatures of shocks, flux ropes, and prominences in coronagraph observations of CMEs. *Sol. Phys.*, **284**, 179–201, 2013, DOI: 10.1007/s11207-012-0084-8.

Wan, W., J. Xiong, Z. Ren, L. Liu, M.L. Zhang, F. Ding, B. Ning, B. Zhao, and X. Yue. Correlation between the ionospheric WN4 signature and the upper atmospheric DE3 tide. *J. Geophys. Res. [Space Phys.]*, **115**, A11303, 2010, DOI: 10.1029/2010JA015527.

Wang, C., G. Rosen, B.T. Tsurutani, O.P. Verkhoglyadova, X. Meng, and A.J. Mannucci. Statistical characterization of ionosphere anomalies and their relationship to space weather events. *J. Space Weather Space Clim.*, **6**, A5, 2016, DOI: 10.1051/swsc/2015046.

Webb, D.F., D.A. Biesecker, N. Gopalswamy, O.C. St. Cyr, J.M. Davila, C.J. Eyles, B.J. Thompson, K.D.C. Simunac, and J.C. Johnston. Using STEREO-B as an L5 Space Weather Pathfinder Mission. *Space Res. Today*, **178**, 10–16, 2010, DOI: 10.1016/j.srt.2010.07.004.

Zhang, Y., and L.J. Paxton. An empirical Kp-dependent global auroral model based on TIMED/GUVI FUV data. *J. Atmos. Sol. Terr. Phys.*, **70 (8–9)**, 1231–1242, 2008, DOI: 10.1016/j.jastp.2008.03.008.

Zhang, J., C. Xin, and Ming-de Ding. Observation of an evolving magnetic flux rope before and during a solar eruption. *Nat. Comm.*, **3**, 747, 2012, DOI: 10.1038/ncomms1753.

Zhao, X., and M. Dryer. Current status of CME/shock arrival time prediction. *Space Weather*, **12 (7)**, 448–469, 2014, DOI: 10.1002/2014SW001060.

Zheng, Y., P. Macneice, D. Odstrcil, M.L. Mays, L. Rastaetter, et al. Forecasting propagation and evolution of CMEs in an operational setting: What has been learned. *Space Weather*, **11 (10)**, 557–574, 2013, DOI: 10.1002/swe.20096.

Cite this article as: Mannucci AJ, Hagan ME, Vourlidas A, Huang CY, Verkhoglyadova OP, et al. Scientific challenges in thermosphere-ionosphere forecasting–conclusions from the October 2014 NASA JPL community workshop. *J. Space Weather Space Clim.*, **6**, E01, 2016, DOI: 10.1051/swsc/2016030.